Biogeosciences Discuss., 10, 9315–9343, 2013
www.biogeosciences-discuss.net/10/9315/2013/
doi:10.5194/bgd-10-9315-2013

Biogeosciences Discussions
Open Access

Southern Hemisphere imprint for Indo–Asian summer monsoons during the last glacial period as revealed by Arabian Sea productivity records

T. Caley[1,2], S. Zaragosi[1], J. Bourget[3], P. Martinez[1], B. Malaizé[1], F. Eynaud[1], L. Rossignol[1], T. Garlan[4], and N. Ellouz-Zimmermann[5]

[1]Univ. Bordeaux, CNRS, EPOC, UMR5805, 33400 Talence, France
[2]Section Climate Change and Landscape Dynamics, Dept. of Earth Sciences, Vrije Universiteit Amsterdam, the Netherlands
[3]School of Earth and Environment, CPGCO2, University of Western Australia, 35 Stirling Highway, Crawley 6009, Australia
[4]Service Hydrographique et Océanographique de la Marine, Cellule Sédimentologie, 13 rue du Chatellier, BP30316 29603 Brest cedex, France
[5]IFPEN, 1 & 4 avenue de Bois Préau, 92852 Rueil-Malmaison, France

Received: 11 May 2013 – Accepted: 26 May 2013 – Published: 11 June 2013

Correspondence to: T. Caley (t.caley@vu.nl)

Published by Copernicus Publications on behalf of the European Geosciences Union.

Abstract

The monsoon is one of the most important climatic phenomena: it promotes inter-hemispheric exchange of energy and affects the economical prosperity of several countries exposed to its seasonal seesaw. Previous studies in both the Indian and Asian monsoon systems have suggested a dominant north hemispheric (NH) control on summer monsoon dynamics at the scale of suborbital-millennial climatic changes, while the forcing/response of Indian and Asian monsoons at the orbital scale remains a matter of debate. Here nine marine sediment cores distributed across the whole Arabian Sea are used to build a regional surface marine productivity signal. The productivity signal is driven by the intensity of Indian summer monsoon winds. Results demonstrate the existence of an imprint of suborbital Southern Hemisphere (SH) temperature changes (i.e., Antarctica) on the Indian summer monsoon during the last glacial period, challenging the traditional and exclusive NH forcing hypothesis. Meanwhile, during the last deglaciation, the NH plays a more significant role. The $\delta^{18}O$ signal recorded in the Asian monsoon speleothem records could be exported by winds from the Indian summer monsoon region, as recently proposed in modelling exercise, explaining the SH signature observed in Asian cave speleothems. Contrary to the view of a passive response of Indian and Asian monsoons to NH anomalies, the present results strongly suggest that the Indo–Asian summer monsoon plays an active role in amplifying millennial inter-hemispheric asymmetric patterns. Additionally, this study helps to decipher the observed differences between Indian and Asian-speleothem monsoonal records at the orbital-precession scale.

1 Introduction

Today, the Arabian Sea is characterized by a high sea surface productivity. Although it is difficult to quantify the preformed O_2/nutrient ratio of Antarctic intermediate waters influencing the Indian sector of the Southern Ocean and its control on the Arabian Sea

BGD
10, 9315–9343, 2013

productivity, the seasonal wind reversal in response to Indian monsoonal dynamics is undoubtedly important for nutrient supply to the sea surface, which modulates productivity and subsurface O_2 demand (Böning and Bard, 2009; Nair et al., 1989). The high surface productivity contributes to generate important biogenic fluxes to the sea floor which, combined with a low supply of oxygen by physical pump, produces and maintains an intense oxygen minimum zone (OMZ) (Sarme, 2002; Böning and Bard, 2009) (Fig. 1). High-resolution studies, based on paleoproductivity proxies, have documented production changes in the area linked to variability in upwelling driven by the summer monsoon (Schulz et al., 1998; Altabet et al., 2002; Ivanochko et al., 2005).

It has been long suggested that the Northern Hemisphere (NH) climate controls the Indo–Asian summer monsoon dynamics at suborbital scale (Schulz et al., 1998; Wang et al., 2001; Altabet et al., 2002; Burns et al., 2003; Rohling et al., 2003; Yuan et al., 2004; Ivanochko et al., 2005; Cosford et al., 2008) based on the apparent similarity of these Indo–Asian record structures at millennial/suborbital-scale with that of Greenland $\delta^{18}O$ ice-core records (NGRIP members, 2004). During warm interstadials of the North Atlantic, the atmosphere can hold more moisture as a result of higher air temperatures. In addition, the duration and intensity of winter snow cover over Asia exerts an important control on the intensity of the summer monsoon (Meehl, 1997). A minority of research results led to a different view and suggested a possible teleconnection between the Asian monsoon and Southern Hemisphere (SH) climatic variations (Cai et al., 2006; Rohling et al., 2009). However, such potential teleconnection for the Indian monsoon system remains unexplored. Comparison between Indo–Asian monsoon records and NH changes are traditionally based on a limited number of study sites (Schulz et al., 1998; Wang et al., 2001; Altabet et al., 2002; Ivanochko et al., 2005). Results are therefore reduced to localised datasets and interpretations with possible influence of regional particularities that can induce signal bias. In addition, the forcing-response relationships of Indo–Asian summer monsoons at the orbital scale also remain a matter of debate (Wang et al., 2001, 2008; Clemens et al., 2003, 2010; Cheng et al., 2009; Caley et al., 2011a, b).

BGD
10, 9315–9343, 2013

Here, we analyse suborbital and orbital marine productivity records, based on bromine (Br) signals obtained by XRF counts, in the Arabian Sea (Fig. 1). Previous study has demonstrated a good correlation between biophilic halogen Bromine (Br) and sedimentary Total Organic Carbon (TOC) of the Arabian Sea (Ziegler et al., 2008). We first demonstrate the dominant role of the Indian summer monsoon in driving the productivity signal recorded. Then, Indian summer monsoon changes during the last 80 kyr are investigated, alongside their link with the Asian monsoon system and the potential control of bipolar (NH/SH) climate variability on monsoon dynamics.

2 Material and methods

2.1 Bromine measurements

Bromine measurements were performed with an Avaatech XRF core scanner. Each core section was scanned every 1 cm (except core MD04-2861 which was scanned every 2 cm) with ionization energy of 10 and 30 kv.

2.2 Organic carbon content

The organic carbon content was determined on dry weight sediment by combustion in an LECO CS 125 analyzer (Cauwet et al., 1990). Samples were acidifed in crucibles with 2N HCl to destroy carbonates, then dried at 60 °C to remove inorganic C and most of the remaining acid and water. The analyses were performed by direct combustion in an induction furnace, and the CO_2 formed was determined quantitatively by infrared absorption.

2.3 Age model

The age model was built with seventeen radiocarbon (^{14}C) control points based on two different hemipelagic cores (MD04-2861 (Caley et al., 2011a) and KS07) (Table 1).

BGD
10, 9315–9343, 2013

Radiocarbon ages were obtained at the "Laboratoire de Mesure du Carbone 14" in Saclay ("SacA") within the framework of the "ARTEMIS" radiocarbon dating project. Radiocarbon dates have been corrected for a marine reservoir effect of 400 yr and calibrated to calendar years using CALIB Rev 6.0.1/Marine04 data set (Bard, 1998; Stuiver, 1998). All ages are given as calendar age (cal. BP). In addition, six *Globorotalia* Events (GEs) control points were used on core MD04-2861 (Caley et al., 2011a). Because downcore bromine signals in each of the nine cores showed similar structure and peaks, all core depths (MD04-2861, KS01-04-05-09-11-12-13) were converted to KS07 core depth by tuning each bromine record to the KS07 bromine record with Analyseries software (Paillard et al., 1996). Core KS07 was chosen as a reference core because (1) the core is entirely composed of hemipelagic sediments providing a continuous record over the last 110 ka BP, and because (2) KS07 was not affected by coring disturbance (piston effect) during the coring procedure. Note that during the tuning procedure, some turbiditic events in cores KS09, KS11, KS12 and KS13 were virtually removed because of their instantaneous depositions, considered at a geological time scale. The stratigraphic data obtained in cores MD04-2861 and KS07 were used to build a polynomial age model based on the common KS07 depth (Fig. 2). The polynomial age model was then applied to the nine cores (in KS07 depth, Fig. 3).

3 Results and discussion

3.1 The Arabian Sea productivity signal

Despite the different locations of the cores in very different water depths and sedimentary environments (i.e., along continental margins, deep sedimentary basin or along the Sheba–Owen–Murray ridges, Fig. 1), the common Br pattern registered across time and across the whole Arabian sea indicates that comparable hydrological and sedimentological processes have driven the export and regional fossilisation of this element (Figs. 1, 3). Paleo-climate marine records used in this study, as well as in

BGD
10, 9315–9343, 2013

previous work (Schulz et al., 1998; Ziegler et al., 2010), are located within, close to, or out of the OMZ (Figs. 1, 5). Therefore, it can be suggested that (1) the dynamics of the OMZ in the past is not the main driver of the Br preservation signals observed in current marine records and (2) the potential effect of bioturbation under the OMZ is weak. After completing a calibration (R^2 = 0.87) with the Total Organic Carbon (TOC) content in the sediment (Fig. 4), bromine (Br) signals obtained by XRF counts can be used as proxies of surface marine productivity changes (Ziegler et al., 2008).

As downcore Br signals at each coring site show very similar structure and events (peaks/troughs), a stack was computed. The stacking procedure smoothes the final signal, but it also reinforces the common down-core pattern and facilitates comparison with other records. For that purpose, each Br signal was resampled with a time step of 200 yr using Analyseries software (Paillard et al., 1996). Following this, each Br signal was normalized into a unit standard deviation change around a zero mean, using (x-mean)/(standard deviation). For the obtained stack (Fig. 3), no significant dilution effect by the input and preservation of biogenic carbonate and terrestrial material can be observed (Fig. S1). In order to compare this reference record with the bipolar climate variability, we used the high-resolution NH NGRIP δ^{18}O ice record from Greenland (NGRIP members, 2004) as well as the SH EPICA Dronning Maud Land (EDML) δ^{18}O ice record from Antarctica (EPICA community members, 2006). The chronology (GICC05) of the NH record has been applied, by methane synchronisation, to the SH record.

3.2 Uncertainties associated to marine, ice and continental records

The GICC05 timescale (NGRIP, apply to EDML) is layer-counted with uncertainty limits which increase with age (errors are cumulative), amounting to about 0.9 % at around 12 kyr BP to about 3.5 % at around 32 kyr B.P (Rasmussen et al., 2006; Anderson et al., 2006). The U-Th age uncertainties for the Dongge and Hulu Cave records remain around 1.5 % (Wang et al., 2001, 2004; Yuan et al., 2004).

BGD
10, 9315–9343, 2013

^{14}C dating of marine cores (0 to 40 kyr) involves uncertainties on the order of several centuries (Table 1). Nonetheless, these uncertainties are probably more important, a couple of hundred years, because of the bioturbation influences that could have mixed information between samples, the microscopic impurities, and the assumptions about the marine reservoir age correction. GEs in core MD04-2861 have radioisotopic age constraints derived from U/Th dates based on speleothem records (Ziegler et al., 2010; Caley et al., 2011a) and assume that Arabian Sea GEs and speleothem events are temporally correlative. All these uncertainties can explain some offsets between records discussed hereafter that increase with age.

3.3 Intermediate water circulation forcing on Arabian Sea productivity

The preformed O_2/nutrient ratio of Antarctic intermediate waters influences the Indian sector and could control Arabian Sea productivity. We focus on the interval 10–40 kyr during the last glacial period, as age models are better constrained within this time interval. High-resolution marine sediments studies demonstrate that increases in intermediate water flow in the Arabian Sea (Jung et al., 2009) and the Indo-southwestern Pacific (Pahnke and Zhan, 2005) occurred in anti-phase with changes in Arabian Sea productivity at the suborbital scale (Fig. 6). Increased ventilation events in the SH coincide with abrupt increase of Antarctic intermediate water (AAIW) renewal in the south west Pacific sector of the Southern Ocean, and are out of phase with Arabian Sea productivity increase. At the orbital scale, previous work has demonstrated that the Br signal was not in phase with increased ventilation revealed by the mid-depth benthic δ^{13}C gradient (Caley et al., 2011a).

Therefore, SH ventilation changes can not be considered as the main driver of productivity changes in the Arabian Sea at the orbital and suborbital scale changes. Indian summer monsoon dynamic seems to be the good candidate to explain the productivity signal recorded.

BGD
10, 9315–9343, 2013

3.4 Atmospheric forcing on Arabian Sea productivity

3.4.1 Suborbital-millennial forcing for Indian summer monsoon

The Arabian Sea Br stack shows suborbital variations that follow similar trends to the millennial-scale signal structure visible in Chinese speleothems and in Greenland/Antarctic δ^{18}O ice-core records (Dansgaard, 1993; Wang et al., 2001; NGRIP members, 2004; EPICA community members, 2006) (Fig. 7). Low Br intensities seem to be recorded during events coinciding with Dansgaard–Oeschger stadials and the Younger Dryas (or during out of phase Antarctic warming), including pronounced events of massive ice-rafted debris deposition in the North Atlantic, the so-called Heinrich events (HEs 1 to 6) (Heinrich, 1988) (Fig. 7).

We focus on the 10–40 kyr interval in order to discuss suborbital-millennial changes during the last glacial period, as age models are better constrained within this time interval (Fig. 2 and 5). Statistical analyses for the interval 16–40 kyr reveal better correlations between the Br stack and the –EDML atmospheric signal ($R^2 = 0.33$ for non tuned records and $R^2 = 0.6$ for tuned records) than between the Br stack and the NGRIP atmospheric signal ($R^2 = 0.02$ for non tuned records and $R^2 = 0.01$ for tuned records) (Table 2). A distinct structure in the Br stack from about 22 to 16 kyr BP is also observed. This is not visible in NGRIP but is similar to that recorded in the –EDML ice record (Fig. 7). In addition a recent high-resolution study in the Arabian Sea, using a reflectance record as a proxy for Indian summer monsoon, indicates some differences with NGRIP (Deplazes et al., 2013). The authors mention that the characteristic sawtooth structure of NGRIP δ^{18}O variability is not a good template for tropical hydroclimate change. Based on our comparison, we note a similar structure between the reflectance record and –EDML from about 22 to 16 kyr BP (Fig. 7). These similarities indicate that SH changes might play an important role in Indian summer monsoon dynamics (Table 2), challenging the traditional views of a strict NH control. Results are congruent with both modern observations (Xue et al., 2004) and high-resolution continental Quaternary records from south-western China (An et al., 2011),

BGD
10, 9315–9343, 2013

which demonstrated that lower Antarctic temperatures lead to a stronger high pressure system over the Mascarene region. Indeed, the Mascarene high is forced by the subsiding branch of the Southern SH Hadley cell owing to the Equator-to-Antarctica temperature gradient. This strengthens the cross-equatorial Somali jet leading to increased intensity of Indian summer monsoons (Xue et al., 2004).

For the interval 10–16 kyr, corresponding to the deglaciation period, the role of NH (correlation with NGRIP signal) becomes more important (Table 2, Fig. 7) as also observed in Caley et al. (2013). When the global ice volume decreases, the continental Indian low-pressure system intensifies rapidly and thus enhances the cross-equatorial monsoon gradient, together with an increased moisture supply from the warming tropical Indian Ocean (An et al., 2011).

3.4.2 Suborbital/millennial Indo–Asian summer monsoons relationship

Recent statistical re-evaluations of the $\delta^{18}O$ signal of Asian speleothems demonstrated that this record contains information linked to SH at sub-orbital scale (Cai et al., 2006; Rohling et al., 2009). Results from this study support the idea that the atmospheric $\delta^{18}O$ signal is exported by the Indian summer monsoon winds towards the Asian monsoon system, as recently showed by numerical modelling (Pausata et al., 2011; Lee et al., 2012), explaining the synchronicity between the Indian and Asian monsoon millennial events (Fig. 7). This is in agreement with modern meteorological data indicating that the two monsoon systems are linked through a common humidity source located in the South Indian Ocean (Ding et al., 2004; Clemens et al., 2010). One implication of this different view of the paradigm for NH-triggered sub-orbital monsoon variability is the active role played by the Indo–Asian monsoon for inter-hemispheric variability, as opposed to a passive response driven by NH-generated anomalies (Cheng et al., 2009; Pausata et al., 2011).

This study argues that the Indo–Asian monsoon can be considered as an amplifier of inter-hemispheric energy transfer at sub-orbital scale during the last glacial period. During a glacial period, the monsoon is weak overall (An et al., 2011). The asynchronous

BGD
10, 9315–9343, 2013

relationship between Antarctic and Greenland millennial-scale temperature changes during the last glacial period has led to the theory that the bipolar seesaw acts to redistribute heat according to the state of the Atlantic Ocean meridional overturning circulation (Crowley, 1992; Broecker, 1998). We propose that atmospheric teleconnection can amplify this process and that the Indo–Asian monsoon plays an important role.

During SH cooling, the monsoon circulation is enhanced with important energy transfers to the NH, which can, in turn, amplify/modulate DO interstadials (Figs. 7 and 8). This atmospheric teleconnection has already been suggested for DO interstadials 12, 8, and 1 (Rohling et al., 2003). Conversely, when the SH temperature increases (AIMs), the reduced Indo–Asian monsoon circulation can constitute a positive feedback to the observed stadials recorded in the NH (Figs. 7 and 8). As atmospheric processes are faster than oceanic processes, the monsoon is an ideal candidate to amplify interhemispheric asymmetric patterns during millennial scale changes.

3.4.3 Orbital forcing for Indo–Asian summer monsoons

Superimposed on the suborbital/millennial dynamics, the external (insolation) forcing contributes to Indo–Asian summer monsoon variability. Differences in the amplitude of millennial events can be observed between Indian and Asian monsoon records (Fig. 7). This could be attributed to local influence on speleothem $\delta^{18}O$ signals, or to superimposed orbital-driven insolation variations. As long as other Asian speleothem records reveal an overall positive signal similarity (Cosford et al., 2008), the observed dissimilarity can be attributed to the effect of orbital variations. Furthermore, previous studies have reported significant differences at the orbital scale between the Indian and Asian monsoon systems (Reichart et al., 1998; Clemens and Prell, 2003; Clemens et al., 2010; Ziegler et al., 2010; Caley et al., 2011a, b).

Considering (1) the time period covered by our productivity stack and (2) that the East-Asian monsoon and Indian monsoon records show a good phase relationship in the obliquity band (Clemens et al., 2010; Caley et al., 2011a, b), we have concentrated our effort on the controversial phase relation observed in the precession band. Different

BGD
10, 9315–9343, 2013

explanations have been put forward for these phase relationship. Reichart et al. (1998) proposed that the Indian summer monsoon was sensitive to late summer insolation forcing (August or September perihelion), based on the observation that the maximum in seasonal biological productivity measured in sediment traps occurs in August and September. However, Clemens and Prell (2003) demonstrate that the late timing of the maximum biological flux within the seasonal cycle is not a synchronous response to late summer insolation forcing and should not be extrapolated to processes operating on orbital time scales. Also, Clemens and Prell (2003) and more recently Caley et al. (2011a) suggested the combined effect of sensitive heating over the Tibetan plateau, which is influenced by ice volume changes, and the latent heat export from the southern Indian Ocean to set the timing of strong Indo–Asian summer monsoons within the precession cycle. Caley et al. (2011a) also demonstrates that the productivity signals in the northern Arabian Sea are mainly controlled by summer monsoon dynamics and not AMOC modulated nutrients at orbital scale changes as hypothesized by Ziegler et al. (2010).

The observed synchronicity between the Indian and Asian monsoon suborbital events was used to advance this debate. Thus, the age model has been refined by tuning the Arabian Sea Br stack to the δ^{18}O millennial events of speleothems (Fig. S2). This method enables the high-precision comparison of the Indian and Asian records over a common and orbital-independent age scale. The signals have then been filtered in the precession band using a Gaussian filter with Analyseries software (Paillard et al., 1996) (Fig. 7). We also apply the same filter to the high resolution Indian summer monsoon record of Deplazes et al. (2013), which is independent of our age model (Fig. 7). Strong differences in the precession band occur over the last 80 kyr (Fig. 3) between Indian and Asian monsoon records, whereas the two independent Indian monsoon records do show the same phasing. A constant gap of 7 kyr on average is observed between the Indian and Asian monsoon records (Fig. 7b), confirming that the previous observed discrepancy (Clemens et al., 2010; Ziegler et al., 2010; Caley et al., 2011a) was not a result of age model problems. The Indian and Asian

BGD
10, 9315–9343, 2013

summer monsoon systems show important linkages at suborbital (this study and Deplazes et al., 2013) and orbital-obliquity timescales (Clemens et al., 2010; Caley et al., 2011a). Therefore, climate processes occurring at the orbital-precession scale, and not directly related to Indo–Asian summer monsoon dynamics, probably account for the observed 7 kyr-gap (Fig. 7b). The influence of seasonality in precipitation amount and isotopic composition recorded by Asian speleothems could constitute a potential explanation (Clemens et al., 2010; Caley et al., 2011a). Modern precipitation within the cave region shows that each season accounts for a certain percentage of annual precipitation with different moisture sources and unique isotopic compositions (Clemens et al., 2010). Following this hypothesis, the SH dynamics could play an important role in controlling orbital-scale Indian summer monsoon dynamics (Clemens and Prell, 2003; Clemens et al., 2010; Caley et al., 2011a) by increasing the latent heat export from the southern Indian Ocean. Alternatively, recent modelling work suggests that ENSO can influence the precession scale variability and explains the phase differences between monsoon proxies, particularly between the northern and southern East–Asian summer precipitation region (Shi et al., 2012).

4 Conclusions

Using nine Bromine records along the Arabian Sea we demonstrate the regional importance of the Indian monsoon, rather than changes in intermediate water circulation at suborbital scales, in driving the recorded productivity signal.

The Indian monsoon records exhibit the imprint of suborbital Southern Hemisphere (SH) temperature dynamic (i.e., Antarctica) during the last glacial period, a pattern also visible in Asian monsoon record. We argue that the Indo–Asian monsoon can therefore be considered as an amplifier of inter-hemispheric energy transfer at sub-orbital scale.

Further work is necessary to better constrain the influence of seasonality and internal feedback on the different monsoonal regions at the precession cycle. Nevertheless, this study demonstrates that the Indo–Asian summer monsoon could be a coupled

BGD
10, 9315–9343, 2013

ocean/atmosphere mechanism capable of amplifying inter-hemispheric asymmetric patterns.

Supplementary material related to this article is available online at: http://www.biogeosciences-discuss.net/10/9315/2013/bgd-10-9315-2013-supplement.pdf.

Acknowledgements. All scientists, technicians and crew members of the R/V *Marion-Dufresne* and *Beautemps Breaupré* are acknowledge for technical assistance during the CHAMAK and Fanindien cruises. The "ARTEMIS" radiocarbon dating project is acknowledged.

The publication of this article is financed by CNRS-INSU.

References

Altabet, M. A., Higginson, M. J., and Murray, D. W.: The effect of millennial-scale changes in Arabian Sea denitrification on atmospheric CO_2, Nature, 415, 159–162, 2002.

An, Z., Clemens, S. C., Shen, J., Qiang, X., Jin, Z., Sun, Y., Prell, W. L., Luo, J., Wang, S., Xu, H., Cai, Y., Zhou, W., Liu, X., Liu, W., Shi, Z., Yan, L., Xiao, X., Chang, H., Wu, F., Ai, L., and Lu, F.: Glacial-interglacial Indian summer monsoon dynamics, Science, 333, 719–723, doi:10.1126/science.1203752, 2011.

Andersen, K. K., Svensson, A., Johnsen, S. J., Rasmussen, S. O., Bigler, M., Röthlisberger, R., Ruth, U., Siggaard-Andersen, M.-L., Steffensen, J. P., Dhal-Jensen, D., Vinther, B. M., and Clausen, H. B.: The Greenland ice core chronology 2005, 15–42 ka, Part 1: constructing the time scale, Quat. Sci. Rev., 25, 3246–3257, 2006.

BGD
10, 9315–9343, 2013

Bard, E.: Geochemical and geophysical implications of the radiocarbon calibration, Geochim. Cosmochim. Ac., 62, 2025–2038, 1998.
Böning, P. and Bard, E.: Millennial/centennial-scale thermocline ventilation changes in the Indian Ocean as reflected by aragonite preservation and geochemical variations in Arabian Sea sediments, Geochim. Cosmochim. Ac., 73, 6771–6788, 2009.
Broecker, W. S.: Paleocean circulation during the last deglaciation: a bipolar seesaw?, Paleoceanography, 13, 119–121, 1998.
Burns, S. J., Fleitmann, D., Matter, A., Kramers, J., and Al-Subbary, A. A.: Indian Ocean climate and an absolute chronology over Dansgaard/Oeschger Events 9 to 13, Science, 301, 1365–1367, 2003.
Cai, Y., An, Z., Cheng, H., Edwards, L. R., Kelly, M. J., Liu, W., Wang, X., and Shen, C. C.: High-resolution absolute-dated Indian Monsoon record between 53 and 36 ka from Xiaobailong Cave, southwestern China, Geology, 34, 621–624, 2006.
Caley, T., Malaizé, B., Zaragosi, S., Rossignol, L., Bourget, J., Eynaud, F., Martinez, P., Giraudeau, J., Charlier, K., and Ellouz-Zimmermann, N.: New Arabian Sea records help decipher orbital timing of Indo-Asian monsoon, Earth Planet. Sc. Lett., 308, 433–444, doi:10.1016/j.epsl.2011.06.019, 2011a.
Caley, T., Malaizé, B., Revel, M., Ducassou, E., Wainer, K., Ibrahim, M., Shoeaib, D., Migeon, M., and Marieu, V.: Orbital timing of the Indian, East Asian and African boreal monsoons and the concept of a "global monsoon", Quaternary Sci. Rev., 30, 3705–3715, doi:10.1016/j.quascirev.2011.09.015, 2011b.
Caley, T., Malaizé, B., Kageyama, M., Landais, A., and Masson-Delmotte, V.: Bi-hemispheric forcing for Indo-Asian monsoon during glacial terminations, Quaternary Sci. Rev., 59, 1–4, 2013.
Cauwet, G., Gadel, F., De Souza Sierra, M. M., Donard, O., and Ewald, M.: Contribution of the Rhone River to org. C inputs to the Northwestern Mediterranean Sea, Cont. Shelf. Res., 10, 1025–1037, 1990.
Cheng, H., Edwards, R. L., Broecker, W. S., Denton, G. H., Kong, X., Wang, Y., Zhang, R., and Wang, X.: Ice age terminations, Science, 326, 248–252, 2009.
Clemens, S. C. and Prell, W. L.: A 350 000 year summer-monsoon multiproxie stack from the Owen ridge, Northern Arabian Sea, Mar. Geol., 201, 35–51, 2003.

BGD
10, 9315–9343, 2013

Clemens, S. C., Prell, W. L., and Sun, Y.: Orbital-scale timing and mechanisms driving Late Pleistocene Indo–Asian summer monsoons: reinterpreting cave speleothem δ^{18}O, Paleoceanography, 25, PA4207, doi:10.1029/2010PA001926, 2010.

Conkright, M. E. and Boyer, T. P.: World Ocean Atlas 2001: Objective Analyses, Data Statistics, and Figures, CD-ROM Documentation, National Oceanographic Data Center, Silver Spring, 2002.

Cosford, J., Qing, H., Yuan, D., Zhang, M., Holmden, C., Patterson, W., and Hai, C.: Millennial-scale variability in the Asian monsoon: evidence from oxygen isotope records from stalagmites in China, Palaeogeogr. Palaeocl., 266, 3–12, 2008.

Crowley, T. J.: North Atlantic deep water cools the Southern Hemisphere, Paleoceanography, 7, 489–497, 1992.

Dansgaard, W., Johnsen, S. J., Clausen, H. B., Dahl-Jensen, D., Gundestrup, N. S., Hammer, C. U., Hvidberg, C. S., Steffensen, J. P., Sveinbjornsdottir, A. E., Jouzel, J., and Bond, G.: Evidence for general instability of past climate from a 250 kyr ice core, Nature, 364, 218–219, 1993.

Deplazes, G., Lückge, A., Peterson, L. C., Timmermann, A., Hamann, Y., Hughen, K. A., Röhl, U., Laj, C., Cane, M. A., Sigman, D. M., and Haug, G. H.: Links between tropical rainfall and North Atlantic climate during the last glacial period, Nat. Geosci., 6, 213–217, doi:10.1038/ngeo1712, 2013.

Ding, Y., Li, C., and Liu, Y.: Overview of the South China Sea monsoon experiment, Adv. Atmos. Sci., 21, 343–360, doi:10.1007/BF02915563, 2004.

EPICA Community Members: One-to-one hemispheric coupling of millennial polar climate variability during the last glacial, Nature, 444, 195–198, 2006.

Garcia, H. E., Locarnini, R. A., Boyer, T. P., and Antonov, J. I.: World Ocean Atlas 2005, vol. 3, Dissolved Oxygen, Apparent Oxygen Utilization, and Oxygen Saturation, NOAA Atlas NESDIS, 63 pp., 2006.

Heinrich, H.: Origin and consequences of cyclic ice rafting in the Northeast Atlantic Ocean during the past 130 000 years, Quaternary Res., 29, 142–152, 1988.

Ivanochko, T. S., Ganeshrama, R. S., Brummer, G.-J. B., Ganssen, G., Jung, S. J. A., Moreton, S. G., and Kroon, D.: Variations in tropical convection as an amplifier of global climate change at the millennial scale, Earth Planet. Sc. Lett., 235, 302–314, 2005.

BGD
10, 9315–9343, 2013

Jung, S. J. A., Kroon, D., Ganssen, G., Peeters, F., and Ganeshrama, R.: Enhanced Arabian Sea intermediate water flow during glacial North Atlantic cold phases, Earth Planet. Sc. Lett., 280, 220–228, doi:10.1016/j.epsl.2009.01.037, 2009.

Laskar, J., Robutel, P., Joutel, F., Gastineau, M., Correia, A. M. C., and Levrard, B.: A long-term numerical solution for the insolation quantities of the Earth, A&A, 428, 261–285, 2004.

Lee, J. E., Risi, C., Fung, I., Worden, J., Scheepmaker, R. A., Lintner, B., and Frankenberg, C.: Asian monsoon hydrometeorology from TES and SCIAMACHY water vapor isotope measurements and LMDZ simulations: implications for speleothem climate record interpretation, J. Geophys. Res., 117, D15112, doi:10.1029/2011JD017133, 2012.

Meehl, G. A.: The south Asian monsoon and the tropospheric biennial oscillation, J. Climate, 10, 1921–1943, 1997.

Nair, R. R., Ittekkot, V., Manganini, S. J., Ramaswamy, V., Haake, B., Degens, E. T., Desai, B. N., and Honjo, S.: Increased particle flux to the deep ocean related to monsoons, Nature, 338, 749–751, 1989.

NGRIP members: High-resolution record of Northern Hemisphere climate extending into the last interglacial period, Nature, 431, 147–151, 2004.

Paillard, D., Labeyrie, L. D., and Yiou, P.: Macintosh program performs time-series analysis, Eas Trans., 77, 379–379, 1996.

Pahnke, K. and Zahn, R.: Southern Hemisphere water mass conversion linked to North Atlantic climate variability, Science, 307, 1741–1746, 2005.

Pausata, F. S. R., Battisti, D. S., Nisancioglu, K. H., and Bitz, C. M.: Chinese stalagmite δ^{18}O controlled by changes in the Indian monsoon during a simulated Heinrich event, Nat. Geosci., 4, 474–480, doi:10.1038/ngeo1169, 2011.

Rasmussen, S. O., Andersen, K. K., Svensson, A. M., Steffensen, J. P., Vinther, B. M., Clausen, H. B., Siggaard-Andersen, M.-L., Johnsen, S. J., Larsen, L. B., Dahl-Jensen, D., Bigler, M., Röthlisberger, R., Fischer, H., Goto-Azuma, K., Hansson, M. E., and Ruth, U.: A new Greenland ice core chronology for the last glacial termination, J. Geophys. Res., 111, D06102, doi:10.1029/2005JD006079, 2006.

Reichart, G. J., Lourens, L. J., and Zachariasse, W. J.: Temporal variability in the northern Arabian Sea oxygen minimum zone (OMZ) during the last 225 000 years, Paleoceanography, 13, 607–621, 1998.

Rohling, E. J., Mayewski, P. A., and Challenor, P.: On the timing and mechanism of millennial-scale climate variability during the last glacial cycle, Clim. Dynam., 20, 257–267, 2003.

BGD
10, 9315–9343, 2013

Rohling, E. J., Liu, Q. S., Roberts, A. P., Stanford, J. D., Rasmussen, S. O., Langen, P. L., and Siddall, M.: Controls on the East Asian monsoon during the last glacial cycle, based on comparison between Hulu Cave and polar ice-core records, Quaternary Sci. Rev., 28, 3291–3302, doi:10.1016/j.quascirev.2009.09.007, 2009.

Sarma, V. V. S. S.: An evaluation of physical and biogeochemical processes regulating perennial suboxic conditions in the water column of the Arabian Sea, Global Biogeochem. Cy., 16, 1082, doi:10.1029/2001GB001461, 2002.

Schlitzer, R.: Ocean Data View, available at: http://odv.awi.de, 2011.

Schulz, H., von Rad, U., and Erlenkeuser, H.: Correlation between Arabian Sea and Greenland climate oscillations of the past 110,000 years, Nature, 393, 54–57, 1998.

Shi, Z., Liu, X., and Cheng, X.: Anti-phased response of northern and southern East Asian summer precipitation to ENSO modulation of orbital forcing, Quaternary Sci. Rev., 40, 30–38, 2012.

Stuiver, M.: INTCAL98 radiocarbon age calibration, 24 000-0 cal BP, Radiocarbon, 40, 1041–1083, 1998.

Wang, Y. J., Cheng, H., Edwards, R. L., An, Z. S., Wu, J. Y., Shen, C.-C., and Dorale, J. A.: A high-resolution absolute-dated late Pleistocene monsoon record from Hulu Cave, China, Science, 294, 2345–2348, 2001.

Wang, Y. J., Cheng, H., Edwards, R. L., Kong, X., Shao, X., Chen, S., Wu, J., Jiang, X., Wang, X., and An, Z.: Millennial and orbital-scale changes in the east Asian monsoon over the past 224 000 years, Nature, 451, 1090–1093, 2008.

Xue, F., Wang, H., and He, J.: Interannual Variability of mascarene high and australian high and their influences on East Asian summer monsoon, J. Meteorol. Soc. Jpn., 82, 1173–1186, 2004.

Yuan, D., Cheng, H., Edwards, R. L., Dykoski, C. A., Kelly, M. J., Zhang, M., Qing, J., Lin, Y., Wang, Y., Wu, J., Dorale, J. A., An, Z., and Cai, Y.: Timing, duration, and transitions of the last interglacial Asian Monsoon, Science, 304, 575–578, 2004.

Ziegler, M., Jilbert, T., de Lange, G. J., Lourens, L. J., and Reichart, G. J.: Bromine counts from XRF scanning as an estimate of the marine organic carbon content of sediment cores, Geochem. Geophy. Geosy., 9, Q05009, doi:10.1029/2007GC001932, 2008.

BGD
10, 9315–9343, 2013

Ziegler, M., Lourens, L. J., Tuenter, E., Hilgen, F., Reichart, G. J., and Weber, N.: Precession phasing offset between Indian summer monsoon and Arabian Sea productivity linked to changes in Atlantic overturning circulation, Paleoceanography, 25, doi:10.1029/2009PA001884, 2010

BGD
10, 9315–9343, 2013

Table 1. ^{14}C dating in core KS07, MD04-2861 (Caley et al., 2011a) and age constrains of GEs in core MD04-2861 (Caley et al., 2011a).

Depth in core KS07 (cm)	Species	Age ^{14}C AMS conv. BP	errors age (cal. yr BP)	Calibrated ^{14}C	errors
0	bulk	2925	30	2713	50
20	bulk	8535	30	9177	121
40	bulk	12 405	40	13 849	124
55	bulk	13 620	50	16 209	630
60	bulk	14 710	50	17 384	335
150	bulk	20 970	80	24 560	356
Depth in core MD04-2861 (cm)	Species	Age ^{14}C AMS conv. BP	errors age (cal. yr BP)	Calibrated ^{14}C	errors
10	bulk	1100	30	658	48
70	bulk	3905	30	3877	96
140	G. dutertrei	6900	35	7417	75
250	G. dutertrei	9845	45	10 757	368
250	G. ruber	10 345	45	11 325	232
340	bulk	14 160	60	16 867	169
450	G. ruber	17 470	70	20 268	212
480	Praeorbulina	18 290	60	21 381	202
500	G. ruber	19 850	70	23 311	291
640	G. ruber	25 170	140	29 597	409
810	G. ruber	34 170	260	38 711	632
Depth in core MD04-2861 (cm)	Globorotalia events			Age (Caley et al., 2011)	
370	GE1			17 400	
800	GE3			39 500	
1090	GE6			64 300	
1330	GE8			85 000	
1430	GE9			103 900	
1470	GE10			110 000	

BGD
10, 9315–9343, 2013

Table 2. Statistical tests with "R" software underlying the coefficient of determination R^2 and P value between productivity records of the Arabian Sea and bipolar climate records (NGRIP and –EDML $\delta^{18}O_{ice}$) for the interval 10–16 and 16–40 kyr. The correlation for the average bromine records, the bromine stack on the original age model (^{14}C and GEs, dots) and tuned bromine stack to NGRIP and –EDML $\delta^{18}O_{ice}$ records are indicated at the end of the Table.

Core	Lat	Lon	Depth	Last 40 kyr resolution (yr)	R^2 –EDML (10–16 kyr)	P value –EDML	R^2 –EDML (16–40 kyr)	P value –EDML	R^2 NGRIP (10–16 kyr)	P value NGRIP	R^2 NGRIP (16–40 kyr)	P value NGRIP
KS01	15.9	55.4	3222	150	0.00	0.90*	0.25	0.00	0.07	0.10*	0.00	0.53*
KS04	16.5	61.0	3994	200	0.32	0.04	0.01	0.40*	0.62	0.00	0.01	0.50*
KS05	19.4	60.8	2710	90	0.41	0.00	0.09	0.00	0.16	0.00	0.03	0.05*
KS07	18.0	58.0	2209	132	0.56	0.00	0.25	0.00	0.27	0.00	0.02	0.03
KS09	21.7	61.1	3185	80	0.64	0.00	0.25	0.00	0.36	0.00	0.02	0.01
KS11	20.2	61.3	4004	65	0.24	0.00	0.20	0.00	0.01	0.50*	0.01	0.01
KS12	20.2	61.5	3726	145	0.02	0.50*	0.36	0.00	0.12	0.10*	0.00	0.40*
KS13	22.3	60.3	2678	50	0.30	0.00	0.20	0.00	0.42	0.00	0.01	0.03
MD04-2861	24.1	63.9	2049	100	0.15	0.00	0.38	0.00	0.12	0.00	0.00	0.40*
NIOP 463 (Ziegler et al., 2010)	22.5	64.0	920	160	0.01	0.70*	0.12	0.00	0.16	0.10*	0.00	0.30*
SO90-111KL (Schulz et al., 1998)	23.1	66.5	775	90	0.00	0.90*	0.36	0.00	0.38	0.00	0.06	0.00
Average Bromine					**0.27**		**0.21**		**0.23**		**0.01**	
Stack Bromine				200	**0.50**	0.00	**0.33**	0.00	**0.43**	0.00	**0.02**	0.10*
Stack Bromine tuned				200	**0.63**	0.00	**0.60**	0.00	**0.48**	0.00	**0.01**	0.80*

* refers to insignificant regressions between records.

BGD
10, 9315–9343, 2013

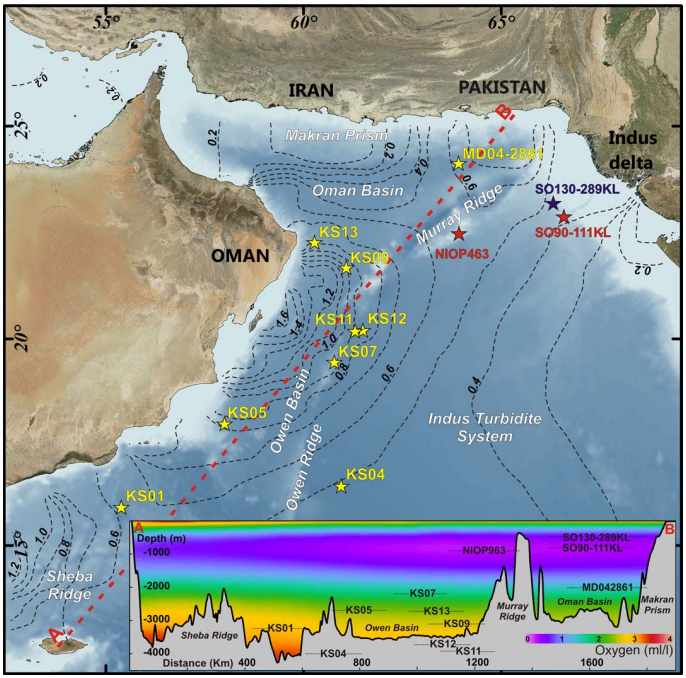

Fig. 1. Core locations in the Arabian Sea with hydrological data corresponding to Indian summer monsoon conditions. The effect of summer monsoon wind-driven upwelling of nutrient-rich subsurface waters is visible through the surface concentration in chlorophyll (black dash lines in $\mu g L^{-1}$; data from July, August, September derived from NOAA NODC WOA01, Conkright and Boyer, 2002). Low supply of oxygen by physical pump, combined with high surface productivity, produce an intense oxygen minimum zone (OMZ) (data for the oxygen profile are derived from the WAO05 (Garcia et al., 2006) and plot using Ocean Data View, Schlitzer, 2011) as visible along the A–B profile. Yellow and red stars indicate the coring sites used in this study and previously published (Schulz et al., 1998; Ziegler et al., 2010), respectively. The blue star indicates the coring site of Deplazes et al. (2013) discussed in this study.

BGD
10, 9315–9343, 2013

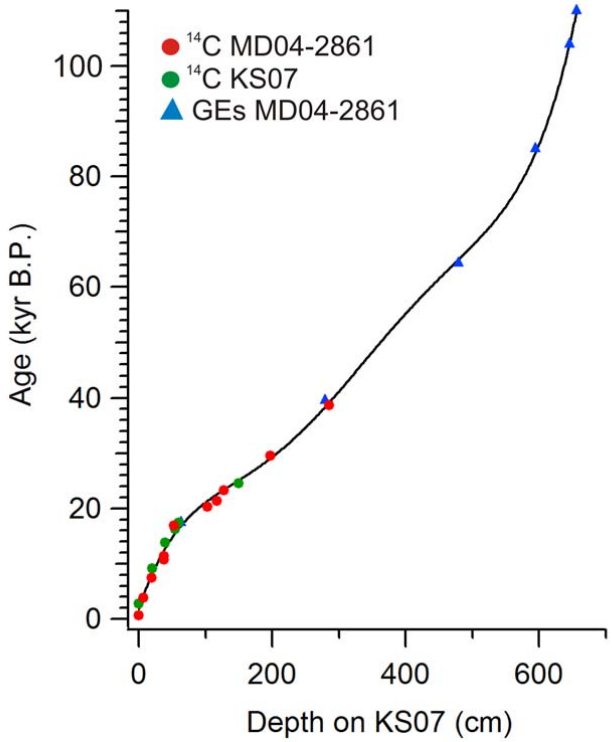

Fig. 2. Age model built with seventeen radiocarbon (^{14}C) control points based on two different hemipelagic cores (MD04-2861 (Caley et al., 2011a) and KS07) and six Globorotalia Events (GEs) control points on core MD04-2861 (Caley et al., 2011a).

BGD
10, 9315–9343, 2013

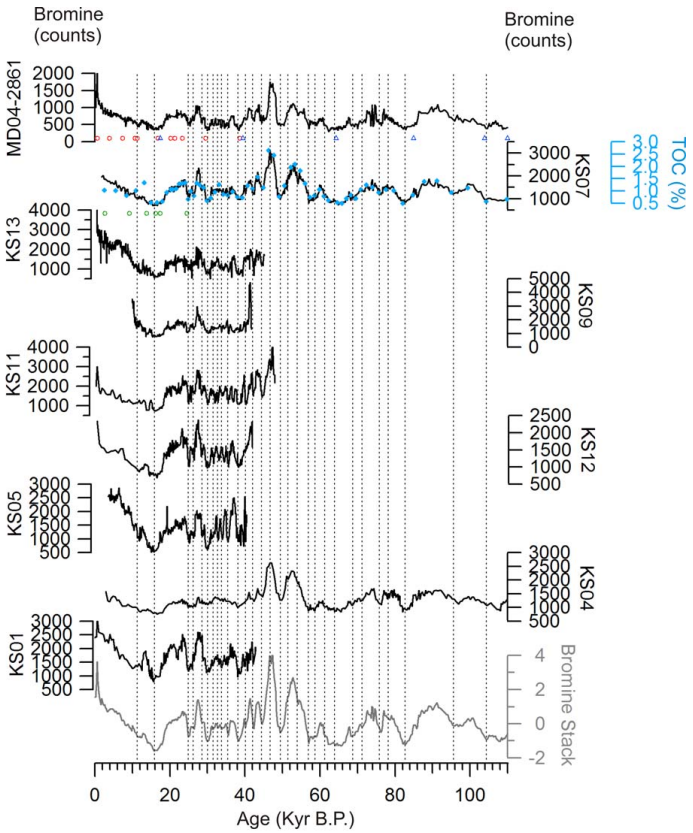

Fig. 3. Bromine signals and accompanying bromine stack for the whole Arabian Sea. All the bromine XRF-count signals obtained for the nine studied cores are visible for the last 110 kyr. For cores MD04-2861 and KS07, age control points are indicated by the red and green circles (^{14}C dates) and blue triangles (GEs). Blue dots for core KS07 refer to Total Organic Carbon (TOC) values. Black dashed lines indicate common events of low bromine values in each record.

BGD
10, 9315–9343, 2013

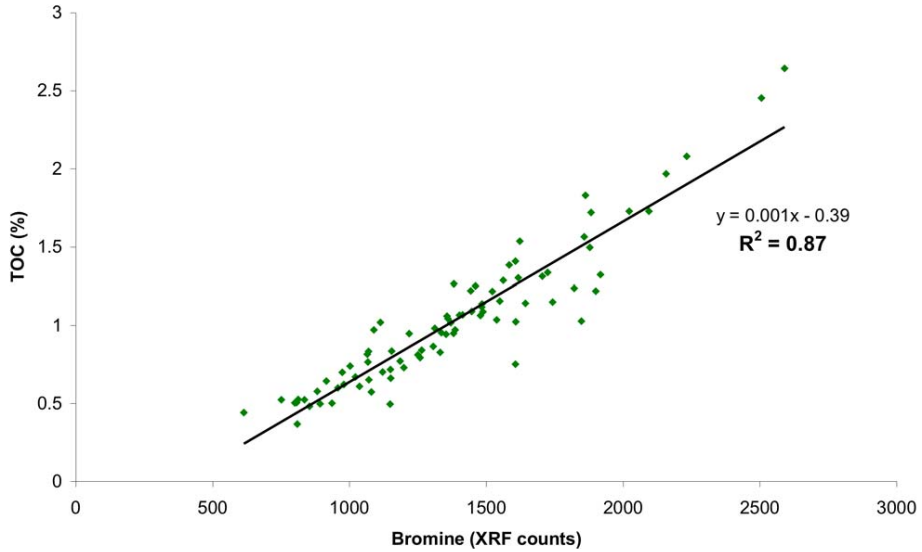

Fig. 4. Relationship between Total Organic Carbon (TOC) (%) and bromine XRF counts for core KS07.

BGD
10, 9315–9343, 2013

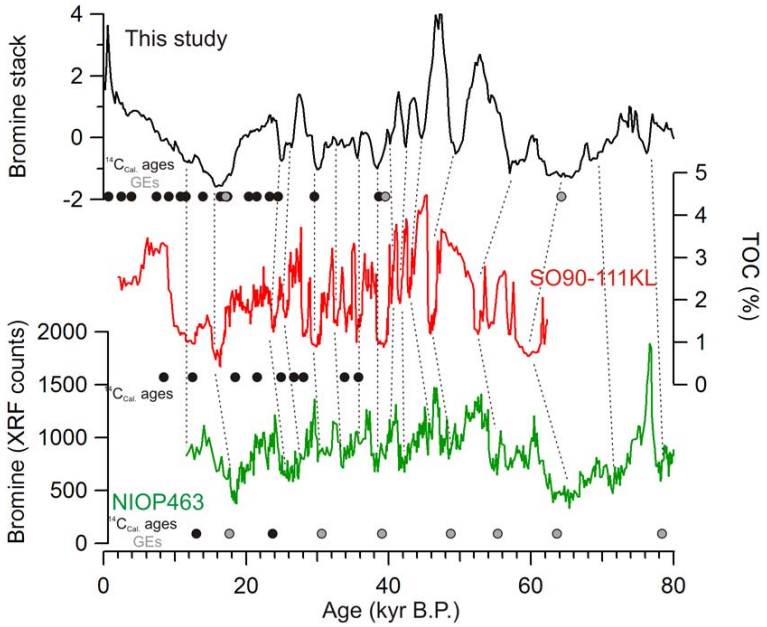

Fig. 5. Relationship between the bromine stack and previous published productivity records in the Arabian Sea. The red curve refers to Total Organic Carbon (TOC) at site SO90-111KL (Schulz et al., 1998) (see Fig. 1 for location). The green curve refers to the bromine stack of core NIOP463 (Ziegler et al., 2010) in the OMZ (Fig. 1). Our bromine stack and TOC record (Schulz et al., 1998) show a very good relationship for suborbital changes until 40 kyr, where the age models are strongly constrain by $^{14}C_{cal}$ control points. From 40 to 80 kyr, both bromine stacks (this study and Ziegler et al., 2010) show a good relationship related to the use of GEs control points. Our records and previous published records show similar signals, despite being located in different areas and at different water depths in the Arabian Sea (Fig. 1). This comparison also confirms the strong relation between TOC and bromine XRF counts in sediment of the Arabian Sea, associated to surface productivity changes.

BGD
10, 9315–9343, 2013

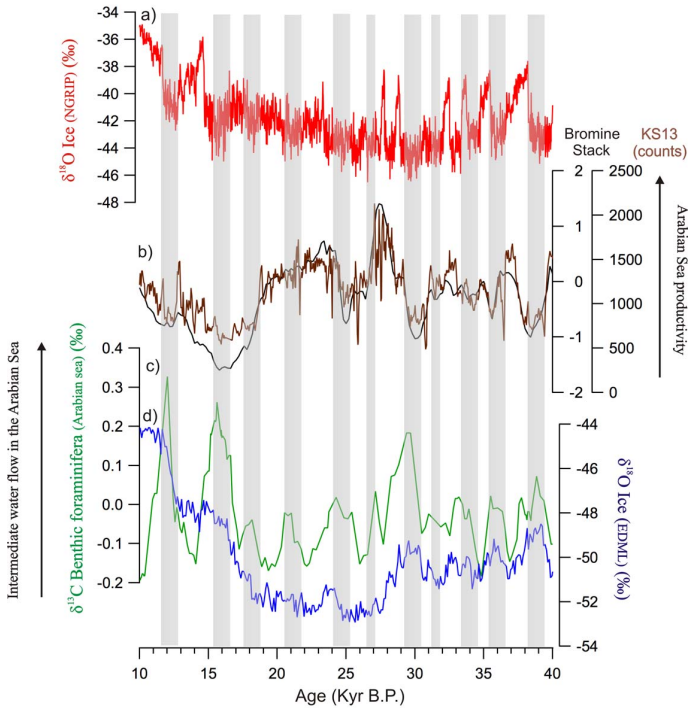

Fig. 6. Comparison between Indian summer monsoon (ISM) changes, intermediate water circulation changes and bipolar climate variability over the last 40 kyr. **(a)** NGRIP $\delta^{18}O_{ice}$ record from Greenland (NGRIP members, 2004). **(b)** Bromine stack as a proxy for ISM. Bromine record of core KS13 has been added for comparison because it has the highest resolution. **(c)** $\delta^{13}C$ as a proxy for intermediate water circulation changes in the Arabian Sea (Jung et al., 2009). **(d)** EPICA Dronning Maud Land (EDML) $\delta^{18}O_{ice}$ record from Antarctica (EPICA community members, 2006). Grey bars indicate increase of intermediate water flow in phase with decrease of productivity in the Arabian Sea.

BGD
10, 9315–9343, 2013

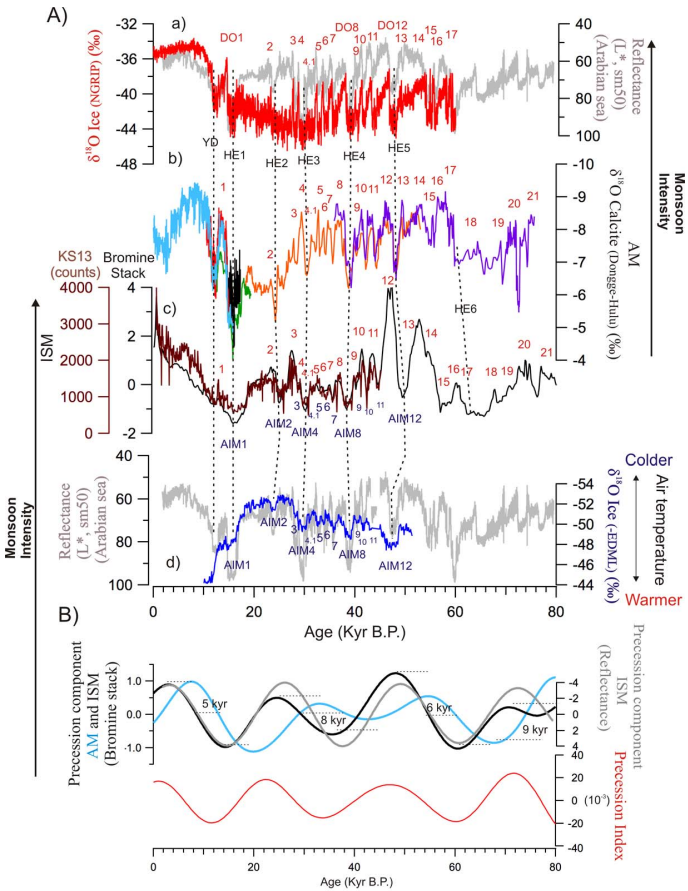

Fig. 7. (Caption on next page.)

BGD
10, 9315–9343, 2013

Southern Hemisphere imprint for Indo–Asian summer monsoons

T. Caley et al.

Fig. 7. Comparison between Indian summer monsoon (ISM) changes, the Asian monsoon (AM) and bipolar climate variability over the last 80 kyr. **(A-a)** NGRIP $\delta^{18}O_{ice}$ record from Greenland (NGRIP members, 2004). The reflectance record as a proxy for Indian summer monsoon (Deplazes et al., 2013) has also been added for comparison. **(A-b)** Chinese speleothem $\delta^{18}O$ calcite record (Wang et al., 2001, 2008) as a proxy for AM. **(A-c)** Bromine stack as a proxy for ISM. Bromine record of core KS13 has been added for comparison because of its highest resolution. **(A-d)** EPICA Dronning Maud Land (EDML) $\delta^{18}O_{ice}$ record from Antarctica (EPICA community members, 2006) (note that the scale is inverted). The reflectance record as a proxy for Indian summer monsoon (Deplazes et al., 2013) has also been added for comparison. Dansgaard–Oeschger (DO) events and Antarctic Isotope Maximums (AIMs) are labelled according to NGRIP members (2004) and EPICA community members (2006). The Younger Dryas and Heinrich events (HEs 1 to 6) are also indicated. **(B)** Precession component of the ISM and AM after tuned the millennial bromine stack events to the Chinese speleothem $\delta^{18}O$ calcite events. The precession component of the reflectance record (Deplazes et al., 2013) on its original age scale is also visible for comparison. Dashed lines indicate a time gap between Indian and Asian records in the precession band. A relatively constant gap of 7 kyr on average is found. The precession index is also visible (Laskar et al., 2004).

BGD
10, 9315–9343, 2013

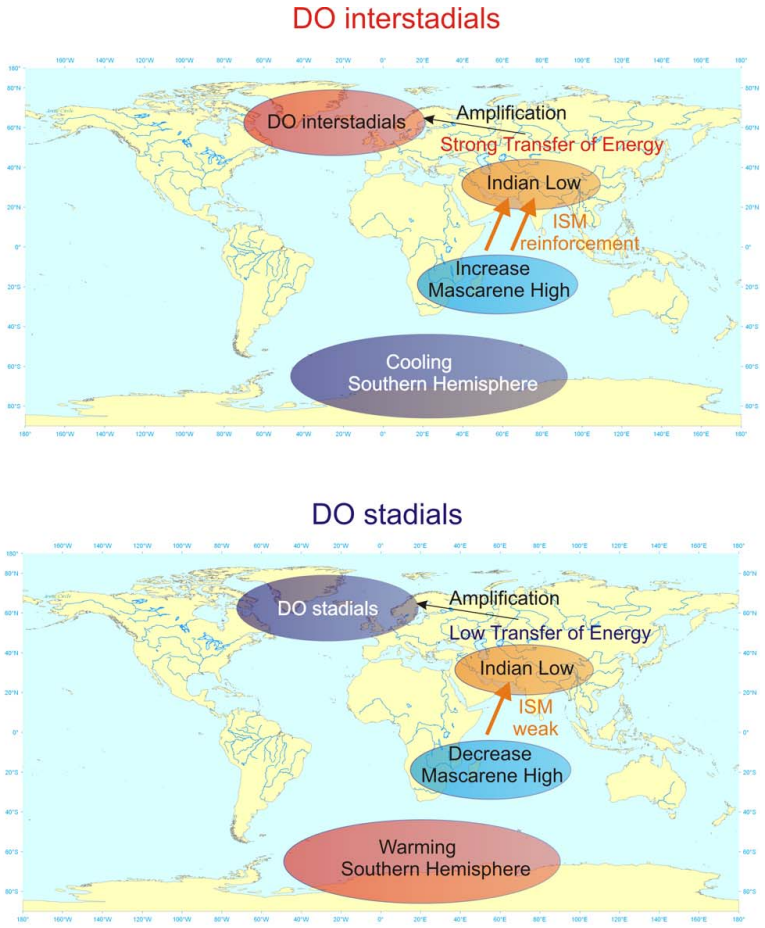

Fig. 8. A conceptual scheme showing how the Indo–Asian monsoon can play an active role to amplify inter-hemispheric energy transfer for sub-orbital changes during the last glacial period.

BGD
10, 9315–9343, 2013